

Technical advances for breast diffusion MR imaging on wide-bore 3T systems

V. S. Deshpande¹, D. J. Wisner², J. W. Grinstead¹, T. Feiweier³, B. N. Joe², and G. A. Laub¹

¹Siemens Medical Solutions USA, Inc., San Francisco, CA, United States, ²Dept. of Radiology and Biomedical Engineering, UCSF, San Francisco, CA, United States,

³Siemens Medical Solutions, Erlangen, Germany

Introduction

Breast MRI has high sensitivity in detecting malignancies, but suffers from only moderate specificity for lesion characterization. Diffusion imaging has shown promise for improved lesion characterization using the apparent diffusion coefficient (ADC) measurements. Results have been reported on 1.5T as well as 3T field strengths^(1,2). Imaging at 3T offers higher SNR, which can translate to higher spatial resolution and better registration with the gradient echo images, thus improving diagnostic utility. However, single-shot EPI (ss-EPI), which is the sequence of choice for breast diffusion imaging, is sensitive to B0 inhomogeneities, which can cause ghosting and spatial distortion artifacts. Moreover, in short and wide bore (70 cm) 3T systems, and thus with the higher likelihood of larger patients, the problems of a non-uniform B0 are exacerbated. In this work, we demonstrate the efficacy of technical improvements in ss-EPI breast diffusion imaging for improving image quality in the presence of B0 imperfections. These improvements are applicable to all field strengths and scanner types.

Methods

Fourteen patients were scanned on a wide-bore 3T Magnetom Verio (Siemens Medical Solutions) with a Sentinelle 8-channel breast coil. An ss-EPI sequence was used for acquiring the diffusion images (Fig. 1). Breast imaging is a challenging application for shimming at 3T and there may be global and focal B0 variations in the FOV. Besides spatial distortions, the B0 variations can compromise fat suppression and phase correction. To improve fat suppression, in addition to using a fat suppression pulse, the slice-select gradient amplitude was reduced for the excitation RF pulse (by using a low bandwidth RF pulse), as compared to the RF pulse used for refocusing. As a result, the spatial shifts for off-resonance species between excitation and refocusing are different, which leads to effective spoiling of the off-resonant spins (Fig. 2). For perfect spoiling under ideal slice profile conditions then:

$$\text{Fatshift}_{90} = \text{Slicethickness} + \text{Fatshift}_{180}$$

If the slice-select gradient is reversed for the refocusing RF pulse⁽³⁾: $\text{Fatshift}_{90} = \text{Slicethickness} - \text{Fatshift}_{180}$

Therefore, use of slice-select gradient reversal increases minimum gradient amplitude required for perfect spoiling. This relaxes requirements of the excitation RF pulse to a relatively larger RF bandwidth, and therefore a shorter duration. A non-linear EPI phase correction was implemented to minimize remnant artifacts. The imaging parameters were as follows: TR/TE = 9000/53 ms, slices = 45, FOV = 153 x 350 mm², matrix = 168 x 192, resolution = 1.8 x 1.8 x 4 mm³, b = 50, 800 s/mm², GRAPPA acceleration = 2, readout bandwidth = 1628 Hz/pixel.

For image assessment, the data were reviewed by an experienced board certified radiologist and the level of artifacts in all the slices was evaluated on a 5-point scale defined as follows: 1: significant artifacts, non-diagnostic; 2: moderate artifact; 3: mild artifacts; 4: minimal artifacts; 5: no artifacts. A Wilcoxon signed rank test was performed to evaluate statistical significance.

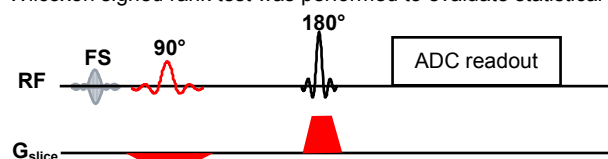


Figure 1. Schematic of the ss-EPI pulse sequence. Note the different slice-select gradient amplitudes and reversed polarities of the excitation and refocusing pulses.



Figure 2. Schematic demonstrating fat suppression using low bandwidth RF pulses and slice-select gradient reversal. S: slice of interest. (a) Different slice-select gradients of excitation and refocusing RF's lead to different spatial shift of excited fat. (b) Slice-select gradient reversal increases spatial separation between the two, thus reducing the requirements of spatial shift required.

Results

Images acquired with a fatsat pulse and different slice-select gradient amplitude + polarity and nonlinear phase correction methods are compared with a standard fat suppression method with linear phase correction (Fig. 3). It is evident that the artifacts are significantly reduced by using the low bandwidth RF pulses and slice-select gradient reversal with a nonlinear EPI phase correction, as shown in Fig. 3. The qualitative reader evaluation also showed similar results, with the improved technique scoring significantly higher. The differences were statistically significant (p=0.001).

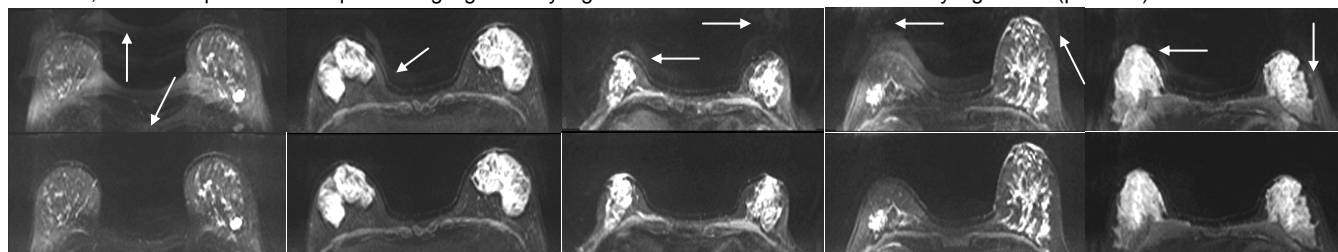


Figure 3. Images comparing **top row:** fatsat pulse + first order phase correction versus **bottom row:** fatsat pulse + low bandwidth RF pulses and slice-select gradient reversal + nonlinear phase correction. There are artifacts in the images in the top row (arrows) that are absent when the improvements are implemented.

Discussion

Single shot EPI techniques suffer from sensitivity to off-resonance. Areas of local off-resonance can contaminate phase correction data and lead to ghosting artifacts as a result. When the fat suppression is sub-optimal, the fat signal not only appears shifted in an EPI image, but it may also corrupt the phase correction and cause ghosting artifacts as a result. These artifacts are compounded if one is using acceleration via parallel imaging, which is essential for EPI to reduce the spatial distortions. In breast imaging, where shimming is very challenging despite localized volume shimming, EPI diffusion can pose problems. Results show that artifacts can be reduced significantly by using different amplitudes and polarities of slice select gradients for excitation and refocusing in a spin echo EPI sequence, and also by using a nonlinear phase correction as opposed to only a first order phase correction. The improvements demonstrated above are promising for improving the image quality and consistency of breast MR diffusion imaging.

References

1. Lo GG, et al. J Comput Assist Tom 2009; 33:63-69
2. El Khouli, RH, et al. Radiology 2010; 256:64-73.
3. Nagy Z, et al. MRM 2008; 60:1256-60